IEEE 1160 93 ■ 4805702 0510359 644 ■

IEEE Standard Test Procedures for High-Purity Germanium Crystals for Radiation Detectors

Circuits and Devices

Communications Technology

Computer

IEEE Nuclear and Plasma Sciences Society

Sponsored by the
Nuclear Instruments and Detectors Committee

Energy and Power

Industrial Applications

Signals and Applications

Standards Coordinating Committees

IEEE Std 1160-1993

IEEE

Published by the Institute of Electrical and Electronics Engineers, Inc., 345 East 47th Street, New York, NY 10017, USA.

May 25, 1993

SH16089

Copyright The Institute of Electrical and Electronics Engineers, Inc.
Provided by IHS under license with IEEE
No reproduction or networking permitted without license from IHS

Not for Resale

IEEE Std 1160-1993

IEEE Standard Test Procedures for High-Purity Germanium Crystals for Radiation Detectors

Sponsor

Nuclear Instruments and Detectors Committee of the IEEE Nuclear and Plasma Sciences Society

Approved March 18, 1993

IEEE Standards Board

Abstract: This standard applies to the measurement of bulk properties of high-purity germanium as they relate to the fabrication and performance of germanium detectors for gamma rays and x rays. Such germanium is monocrystalline and has a net concentration of fewer than 10^{11} electrically active impurity center per cm^3, usually on the order of 10^{10} cm^{-3}.
Keywords: high-purity germanium (HPGe), radiation detectors

The Institute of Electrical and Electronics Engineers, Inc.
345 East 47th Street, New York, NY 10017-2394, USA

Copyright © 1993 by the Institute of Electrical and Electronics Engineers, Inc.
All rights reserved. Published 1993. Printed in the United States of America

ISBN 1-55937-298-2

No part of this publication may be reproduced in any form, in an electronic retrieval system or otherwise, without the prior written permission of the publisher.

Copyright The Institute of Electrical and Electronics Engineers, Inc.
Provided by IHS under license with IEEE
No reproduction or networking permitted without license from IHS

Not for Resale

IEEE Standards documents are developed within the Technical Committees of the IEEE Societies and the Standards Coordinating Committees of the IEEE Standards Board. Members of the committees serve voluntarily and without compensation. They are not necessarily members of the Institute. The standards developed within IEEE represent a consensus of the broad expertise on the subject within the Institute as well as those activities outside of IEEE that have expressed an interest in participating in the development of the standard.

Use of an IEEE Standard is wholly voluntary. The existence of an IEEE Standard does not imply that there are no other ways to produce, test, measure, purchase, market, or provide other goods and services related to the scope of the IEEE Standard. Furthermore, the viewpoint expressed at the time a standard is approved and issued is subject to change brought about through developments in the state of the art and comments received from users of the standard. Every IEEE Standard is subjected to review at least every five years for revision or reaffirmation. When a document is more than five years old and has not been reaffirmed, it is reasonable to conclude that its contents, although still of some value, do not wholly reflect the present state of the art. Users are cautioned to check to determine that they have the latest edition of any IEEE Standard.

Comments for revision of IEEE Standards are welcome from any interested party, regardless of membership affiliation with IEEE. Suggestions for changes in documents should be in the form of a proposed change of text, together with appropriate supporting comments.

Interpretations: Occasionally questions may arise regarding the meaning of portions of standards as they relate to specific applications. When the need for interpretations is brought to the attention of IEEE, the Institute will initiate action to prepare appropriate responses. Since IEEE Standards represent a consensus of all concerned interests, it is important to ensure that any interpretation has also received the concurrence of a balance of interests. For this reason IEEE and the members of its technical committees are not able to provide an instant response to interpretation requests except in those cases where the matter has previously received formal consideration.

Comments on standards and requests for interpretations should be addressed to:

Secretary, IEEE Standards Board
445 Hoes Lane
P.O. Box 1331
Piscataway, NJ 08855-1331
USA

IEEE Standards documents are adopted by the Institute of Electrical and Electronics Engineers without regard to whether their adoption may involve patents on articles, materials, or processes. Such adoption does not assume any liability to any patent owner, nor does it assume any obligation whatever to parties adopting the standards documents.

Copyright The Institute of Electrical and Electronics Engineers, Inc.
Provided by IHS under license with IEEE
No reproduction or networking permitted without license from IHS
Not for Resale

Introduction

(This introduction is not a part of IEEE Std 1160-1993, IEEE Standard Test Procedures for High-Purity Germanium Crystals for Radiation Detectors.)

The subject of this standard is the measurement of the bulk properties of high-purity germanium (HPGe) intended for use in detectors of ionizing radiation.

Detector manufacturers desire numerical data that can be used to predict the performance of a detector having approximately coaxial geometry. However, because of the many variations in the physical characteristics, the final detector performance cannot be fully predicted from the crystal manufacturers' measurements. This standard defines terminology and measuring techniques for determining and communicating key crystal parameters.

At the time that this standard was approved, the Nuclear Instruments and Detectors Committee of the IEEE Nuclear and Plasma Sciences Society had the following membership:

Sanford Wagner, *Chair*
Louis Costrell, *Sectretary*

M. L. Bauer
J. G. Bellian
J. A. Coleman
L. S. Darken
W. K. Dawson
J. Detko
E. Fairstein
F. S. Goulding
R. M. Keyser
F. A. Kirsten
G. F. Knoll
H. W. Kraner
G. L. Miller
D. E. Persyk
P. L. Phelps
D. E. Stilwell
K. L. Swinth
M. P. Unterweger
F. J. Walter

L. S. Darken served as project leader for the development of this standard. Other contributors were P. Clauws, L. Van Goethem, and E. E. Haller.

The American National Standards Committee on Nuclear Instruments (N42), at the time it approved this standard, had the following representatives:

Louis Costrell, *Chairman* **Linda A. Gargiulo,** *Secretary*

Organization Represented	*Name of Representative*
American Conference of Governmental Industrial Hygenists	Jesse Lieberman
Battelle Pacific Northwest Laboratories	J. M. Selby
Health Physics Society	J. B. Horner Kuper
	J. M. Selby *(Alt.)*
Institute of Electrical and Electronic Engineers	Louis Costrell
	Juilian Forster *(Alt.)*
	A. J. Spurgin *(Alt.)*
Lawrence Berkely Laboratory	E. J. Lampo
Lawrence Livermore National Laboratory	P. L. Phelps
Oak Ridge National Laboratory	H. R. Brashear
U. S. Department of the Army	Edward Groeber
U. S. Department of Commerce, NIST	Louis Costrell
U. S. Department of Energy, OHER/PCRSD	Gerald Goldstein
U. S. Federal Emergency Management Agency	C. R. Siebentritt
U. S. Nuclear Regulatory Commission	E. C. Wenzinger
Members-at-Large	J. G. Bellian
	E. A. Corte
	J. M. Gallagher
	J. E. McLaughlin
	D. A. Mack
	E. J. Vallario
	Sanford Wagner

Copyright The Institute of Electrical and Electronics Engineers, Inc.
Provided by IHS under license with IEEE
No reproduction or networking permitted without license from IHS
Not for Resale

The following persons were on the balloting committee that approved this document for submission to the IEEE Standards Board:

M. L. Bauer
J. G. Bellian
J. A. Coleman
L. Costrell
L. S. Darken
W. K. Dawson
J. Detko
E. Fairstein
F. S. Goulding
R. M. Keyser
F. A. Kirsten
G. F. Knoll
H. W. Kraner
G. L. Miller
D. E. Persyk
P. L. Phelps
D. E. Stilwell
K. L. Swinth
S. Wagner
F. J. Walter

When the IEEE Standards Board approved this standard on Sept. 17, 1992, it had the following membership:

Marco Migliaro, *Chair* **Donald C. Loughry,** *Vice Chair*

Andrew G. Salem, *Secretary*

Dennis Bodson
Paul L. Borrill
Clyde Camp
Donald C. Fleckenstein
Jay Forster*
David F. Franklin
Ramiro Garcia
Thomas L. Hannan
Donald N. Heirman
Ben C. Johnson
Walter J. Karplus
Ivor N. Knight
Joseph Koepfinger*
Irving Kolodny
D. N. "Jim" Logothetis
Lawrence V. McCall
T. Don Michael*
John L. Rankine
Wallace S. Read
Ronald H. Reimer
Gary S. Robinson
Martin V. Schneider
Terrance R. Whittemore
Donald W. Zipse

*Member Emeritus

Also included are the following nonvoting IEEE Standards Board liaisons:

Satish K. Aggarwal
James Beall
Richard B. Engelman
David E. Soffrin
Stanley Warshaw

Adam Sicker
IEEE Standards Project Editor

Copyright The Institute of Electrical and Electronics Engineers, Inc.
Provided by IHS under license with IEEE
No reproduction or networking permitted without license from IHS
Not for Resale

Contents

CLAUSE PAGE

1. Overview ... 1

1.1 Scope ... 1
1.2 Purpose ... 1

2. References ... 2

3. Letter symbols ... 2

4. Introduction ... 3

5. Sample preparation and measurement of net electrically active impurity concentration $|N_A - N_D|$ ... 4

5.1 Sample preparation for van der Pauw measurements ... 4
5.2 Measurement and analysis ... 6
5.3 Spatial dependence of $(N_A - N_D)$ ... 11

6. Deep-level transient spectroscopy (DLTS) for the characterization of point-defect trapping centers (N_T) ... 13

6.1 Equipment ... 14
6.2 Sample selection and preparation for DLTS ... 15
6.3 Measurement procedure ... 15
6.4 Majority-carrier deep levels in p-type HPGe ... 19
6.5 Majority-carrier deep levels in n-type HPGe ... 20
6.6 Reporting ... 20

7. Crystallographic properties ... 20

7.1 Crystallographic orientation ... 20
7.2 Sample preparation ... 20
7.3 Reporting ... 22

8. Bibliography ... 22

FIGURES

Figure 5.2 $f(R_{AB,CD}/R_{BC,DA})$ vs. $R_{AB,CD}/R_{BC,DA}$ ... 8
Figure 5.3 Factor r for n-type HPGe, two crystallographic orientations ... 11
Figure 5.4 Factor r for p-type HPGe ... 11
Figure 6.1 DLTS waveforms and gate timing ... 13
Figure 6.2 $\Delta V_c/V_p$ waveforms ... 18

TABLES

Table 1 Majority-carrier deep levels in p-type HPGe ... 19

Copyright The Institute of Electrical and Electronics Engineers, Inc.
Provided by IHS under license with IEEE
No reproduction or networking permitted without license from IHS
Not for Resale

CLAUSE PAGE

Annex A 24
Table A1 Round-robin measurements of n-type sample 25
Table A2 Round-robin measurements of p-type sample 26
Table A3 Magnetic fields used for measurements and *r* values for n-type and p-type HPGe .. 26
Table A4 Average values and standard deviations, whole-slice measurements 27
Table A5 Supplementary data, n-type slice—laboratory #4, procedure B 27
Table A6 p-Type data: direction of transient 28
Table A7 Averages for the measured drift mobility in units of 10^4 cm^2 V^{-1}s^{-1} 29

Copyright The Institute of Electrical and Electronics Engineers, Inc.
Provided by IHS under license with IEEE
No reproduction or networking permitted without license from IHS
Not for Resale

IEEE Standard Test Procedures for High-Purity Germanium Crystals for Radiation Detectors

1. Overview

1.1 Scope

This standard applies to the measurement of bulk properties of high-purity germanium as they relate to the fabrication and performance of germanium detectors for gamma rays and x rays. Such germanium is monocrystalline and has a net concentration of fewer than 10^{11} electrically active impurity centers per cm^3, usually on the order of 10^{10} cm^{-3}. Test and measurement procedures for fabricated germanium detectors are given in IEEE Std 325-1986 and IEEE Std 759-1984.

1.2 Purpose

The purpose of this standard is to establish uniform procedures for measurements and analyses in the determination and reporting of bulk properties relevant to germanium radiation detector fabrication and performance. These properties are net electrically active impurity concentrations, $|N_A - N_D|$, the concentration of isolated defects with deep electronic levels N_T, and certain crystallographic properties. The techniques described herein are those that have found general use in the industry, are practical, and provide verifiable and desired information to the detector fabricator.

As an aid to the reader, an annex is included for background material. Paragraph numbers in the annex are prefixed by the letter "A," while the numerical parts of the numbers correspond to those in the main body of the text to which they pertain.

Not all tests described herein are mandatory; however, any tests that are intended to conform to this standard shall be performed according to its provisions.

Mandatory procedures are designated by the word "shall." Recommended procedures are designated by the words "should" or "recommended." Optional procedures are designated by the word "may."

Copyright The Institute of Electrical and Electronics Engineers, Inc.
Provided by IHS under license with IEEE
No reproduction or networking permitted without license from IHS
Not for Resale

2. References

This document shall be used in conjunction with the standards listed below. References to material appearing in journals and in other publications are listed in clause 8.

IEC 759 (1983), Standard test procedures for semiconductor X-ray energy spectrometers.[1]

IEC 973 (1989), Test procedures for germanium gamma-ray detectors.

IEEE Std 325-1986, IEEE Standard Test Procedures for Germanium Gamma-Ray Detectors (ANSI).[2]

IEEE Std 759-1984, IEEE Standard Test Procedures for Semiconductor X-Ray Energy Spectrometers (ANSI).

3. Letter symbols

Frequently used letter symbols are defined below. Infrequently used symbols are defined where they are introduced in the text.

B	magnetic flux density in tesla (see T)
C	coulombs
C	capacitance in farads
C_d	capacitance of the depleted region in a diode
DLTS	deep-level transient spectroscopy
Δ	change in
e	electronic charge, $1.60 \cdot 10^{-19}$ coulombs
e_r	emission rate from a localized electronic level in s^{-1}
exp (z)	base of the natural logarithms (2.728) to the exponent, z
E	energy associated with an electronic level in the band gap
f	frequency in hertz
HPGe	high-purity germanium
k	Boltzman's constant, $8.617 \cdot 10^{-5}$ eV K^{-1}
K	kelvin
LN	liquid nitrogen
$N_A - N_D$ [3]	net electrically active impurity concentration per cm^3
N_T	deep-level impurity-center concentration per cm^3
Ω	ohm(s)
r	constant associated with measurement of $\lvert N_A - N_D \rvert$ by Hall effect
R	resistance in ohms
R_H	Hall coefficient in cm^3 C^{-1}
ρ	resistivity in $\Omega \cdot$ cm
s	seconds
t	time in seconds

[1]IEC publications are available from IEC Sales Department, Case Postale 131, 3 rue de Varembé, CH-1211, Genève 20, Switzerland/Suisse. IEC publications are also available in the United States from the Sales Department, American National Standards Institute, 11 West 42nd Street, 13th Floor, New York, NY 10036, USA.

[2]IEEE publications are available from the Institute of Electrical and Electronics Engineers, Service Center, 445 Hoes Lane, P.O. Box 1331, Piscataway, NJ 08855-1331, USA.

[3]The sign of the quantity indicates the type of carrier (n or p). Where only the magnitude is required, the expression will appear as $\lvert N_A - N_D \rvert$.

Copyright The Institute of Electrical and Electronics Engineers, Inc.
Provided by IHS under license with IEEE
No reproduction or networking permitted without license from IHS Not for Resale

IEEE 1160 93 ■ 4805702 0510368 657 ■

T	temperature in kelvins
T	tesla (one T = 10^4 gauss)
τ	emission time in seconds
μ	drift mobility in $cm^2\ V^{-1}\ s^{-1}$
μ_H	Hall mobility in $cm^2\ V^{-1}\ s^{-1}$
μ_n	electron drift mobility ($cm^2\ V^{-1}\ s^{-1}$) in a semiconductor crystal
μ_p	hole drift mobility ($cm^2\ V^{-1}\ s^{-1}$) in a semiconductor crystal
V	volt(s)
V_p	pulse amplitude (in volts) in deep-level transient spectroscopy
V_r	reverse bias in volts
ω	$2\pi f$ (see f)
W_p	pulse duration (in seconds) in deep-level transient spectroscopy

4. Introduction

Germanium fulfilling the necessary size and purity requirements for high-purity germanium (HPGe) detectors of ionizing radiation presents special problems in characterization resulting from the high resistivity of the material (~10 kΩ · cm at 77 K), from the degree of impurity compensation that can be encountered, and from difficulties in suitably describing the distribution in the large volume that may form a single device (hundreds of cm^3). Material properties of HPGe have been reviewed in [B7] and [B10]. Other publications are also highly relevant. Existing standards are useful, but are not focused on the problems mentioned above.

One of the most important characteristics of HPGe is the net electrically active impurity concentration, $|N_A - N_D|$, because it determines the depletion voltage required for an operating detector. Although, in principle, the concentration can be extracted from a C^{-2} vs. V plot for a diode fabricated from the material to be characterized, such measurements may not readily yield carrier type, do not quantify nonuniformity, and are more time consuming than other techniques. The usual practice has been to determine $(N_A - N_D)$, with the sign indicating n-type or p-type on the basis of transport measurements using the van der Pauw technique (see [B25]) on lamellar samples immersed in liquid nitrogen (LN).

In the van der Pauw technique, $|N_A - N_D|$ can be computed either from the resistivity, ρ, or from the Hall coefficient, R_H. These, in turn, must be computed from a series of electrical measurements made on the sample.

Measurements made for the determination of ρ are made in the absence of a magnetic field; those for R_H are made with and without the field. The magnetic field, when used, must be oriented orthogonally to the plane of the sample. Details of the measurements are given in 5.2.4 and 5.2.5. The information so obtained also leads to the determination of charge mobility through the crystal.

This standard addresses procedures for characterizing HPGe in three essential areas: net impurity concentration, deep-level trap concentration, and crystallographic quality. Details of sample preparation and the measurement procedures for the determination of $|N_A - N_D|$ are given in clause 5 (see also [B2], Section 63042); the determination of deep-level trap concentration by deep-level transient spectroscopy (DLTS) is covered in clause 6 (see also [B4]); and crystallographic properties are covered in clause 7 (see also [B1] and [B3]).

Because the determination of $|N_A - N_D|$ is critically dependent on sample preparation, a round-robin test was conducted among four laboratories on a set of samples processed by the procedures described in clause 5. The findings are reported in annex A.

Copyright The Institute of Electrical and Electronics Engineers, Inc.
Provided by IHS under license with IEEE
No reproduction or networking permitted without license from IHS

Not for Resale

5. Sample preparation and measurement of net electrically active impurity concentration $|N_A - N_D|$

The size and shape of a sample upon which measurements will be made depends on the exact purpose of the test. Some characteristics, however, are common to all samples:

a) Samples shall be lamellar, with the shortest linear dimension along a face being at least three times greater than the thickness.
b) From the standpoint of measurement theory, samples may be square, rectangular, or circular; geometric perfection is not required.
c) Surface roughness and strains (such as those caused by lapping) shall be removed by polish etching.
d) Four contacts shall be attached, usually on the corners of square samples or at ≈90° spacing on circular samples.

With regard to etching, the surface type (n or p) and the surface stability usually are determined by the details of the wet-chemical processing and the subsequent ambient conditions. Surface type and uniformity may be affected by improper handling. Carriers at an accumulated surface may contribute to conduction. If the surface is inverted, depletion from it will reduce the effective sample thickness. The purer the sample, the more important those effects become and the more important the details of the handling become. For very pure material ($<10^{10}$ cm^{-3}), specialized etch and quench procedures may be required to achieve consistently satisfactory results, particularly for n-type material.

Further details are given in the following subclauses.

5.1 Sample preparation for van der Pauw measurements

As stated earlier, accuracy in the determination of $|N_A - N_D|$ is critically dependent upon sample preparation, which must be carried out with great care.

5.1.1 Equipment

Required equipment are:

a) A string saw or diamond saw.
b) Supplies of semiconductor-grade reagents and access to a vented laboratory hood and sink.
c) The surfaces of the sample must be etched in a way that ensures acid contact on all surfaces; a beaker with a waffled bottom is useful for the purpose. The size of the beaker is important because self heating occurs during the etching process. If the beaker is too large, the reaction will proceed too slowly and a wasteful amount of reagent will be necessary. If the beaker is too small, the reaction will proceed too violently. The optimum size is slightly wider than the sample and deep enough to allow the surface of the etchant to be 1 to 2 cm above the top of the sample.

5.1.2 Dimensions and provisions for contacts

Samples may be cut and fashioned with a string saw or diamond-blade saw. The minimum lateral dimension of a sample used for determining $|N_A - N_D|$ shall exceed three sample thicknesses.

For small samples, squares (or rectangles) are the easiest to form. They should be 1 to 2 cm on a side. If contacts are made at the corners, which is the preferred practice, the corners shall be beveled the minimum amount necessary for stable physical contact [~1 mm bevels, see figure 5.1 a)].

Copyright The Institute of Electrical and Electronics Engineers, Inc.
Provided by IHS under license with IEEE
No reproduction or networking permitted without license from IHS Not for Resale

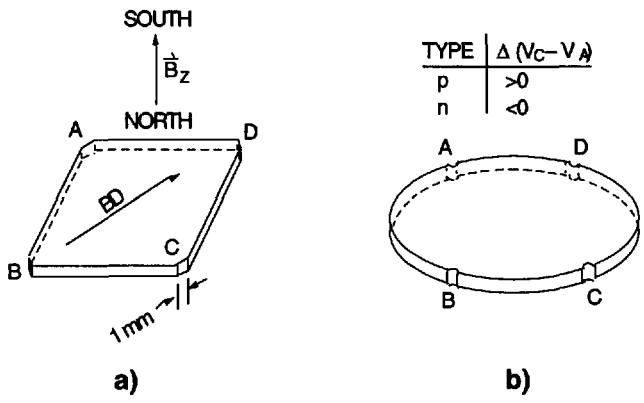


Figure 5.1—Samples: a) square, b) circular

For whole-slice samples, the contacts should be made ~90° apart around the perimeter, again minimizing contact width. To penetrate the as-grown skin, nicks (indentations) may be cut into the slice at the points where the contacts are to be made [see figure 5.1 b)].

The samples shall be etched before applying contacts. Material comprising the contacts is listed in the last step of each of the etching procedures.

5.1.3 Etching

Three chemical procedures for sample preparation are listed below: A, B, and C. All have been tested. Procedure A is preferred, but the use of procedure B avoids mixing acid with methanol and therefore presents fewer environmental problems. The procedure ultimately used, however, should be the one that yields the most accurate prediction of the characteristics of completed detectors.

Semiconductor-grade reagents shall be used. See 5.1.1 for the type of beaker to use.

5.1.3.1 Procedure A

a) If necessary, clean the sample with methanol or deionized water to remove residual contact metal or other impurities. Allow to dry.

b) Prepare chemical polish etch: three parts HNO_3 (70% by weight) to one part HF (49% by weight).

c) If the sample already has a polished surface, etch for 45 s while agitating lightly. The etchant should change from clear to a light green color and should exhibit light bubble formation. If the sample has a sawed or lapped surface, etch for 3 min, agitating lightly or until a vigorous boiling-like reaction begins.

d) Quench rapidly with semiconductor-grade methanol. Rinse rapidly and thoroughly in methanol without exposing the sample to air long enough for it to dry. Residual methanol should be thoroughly decanted from the beaker before the last rinse.

e) Handling only with clean tweezers, dry the sample with a stream of clean dry nitrogen gas.

f) At room temperature, apply four contacts with a eutectic mixture of either Ga-In or Hg-In.

The sample is now ready for measurement.

Copyright The Institute of Electrical and Electronics Engineers, Inc.
Provided by IHS under license with IEEE
No reproduction or networking permitted without license from IHS
Not for Resale

5.1.3.2 Procedure B

a) If necessary, clean the sample with methanol or deionized water to remove residual contact metal or other impurities. Allow to dry.
b) Prepare chemical polishing etch: two parts HNO_3 (70% by weight) to one part HF (49% by weight).
c) Etch for ≈30 s after the mixture begins to react vigorously (intense brown color, large bubbles, and brown nitric oxide fumes). The sample shall be agitated during the reaction to ensure homogeneous etching.
d) Slowly quench the reaction with deionized water (1 to 2.5 L/min) for 15 to 30 s. The sample shall not be exposed to air.
e) Thoroughly clean the sample by flushing with deionized water for ≈1min.
f) Remove the sample with tweezers and immerse in methanol for ≈1min.
g) Handling only with clean tweezers, dry the sample with filter paper or with a stream of clean dry nitrogen gas.
h) At room temperature, apply four contacts with a eutectic mixture of either Ga-In or Hg-In.

The sample is now ready for measurement.

5.1.3.3 Procedure C

a) If necessary, clean the sample with methanol or deionized water to remove residual contact metal or other impurities. Allow to dry.
b) Prepare a stock solution of chemical polishing etch: seven parts HNO_3 (70% by weight), one part red fuming HNO_3, two parts HF (49% by weight). Let age for at least one day.
c) For previously etched samples, tilt slowly back and forth for ≈1min. For lapped samples, tilt slowly back and forth for ≈2 min.
d) Quench the polishing solution with large quantities of fresh semiconductor-grade methanol.
e) Rinse with methanol from a spray bottle.
f) Handling only with clean tweezers, dry the sample with a stream of clean dry nitrogen gas.
g) At room temperature, apply four contacts with a eutectic mixture of Ga-In.

The sample is now ready for measurement.

5.2 Measurement and analysis

A general description of how the net electrically active impurity concentration, $|N_A - N_D|$, is determined is given in clause 4. Details are given below for a square sample with four contacts, A through D, [see figure 5.1 a); note that the contacts are labeled in counterclockwise order]. While two separate quantities must be determined, ρ and R_H, all of the measurements shall be made and recorded in one continuous session. As part of the test, the current shall be reversed and the measurements repeated. Also, the measurements shall be repeated with the current increased by a factor of 10. The purpose of the reversals and current increase is to uncover faults in the measuring instruments or in the preparation of the samples (see 5.2.6).

5.2.1 Equipment

The following equipment are required:

a) A suitable container for immersing the sample in LN during the measurement
b) A constant-current source
c) A voltmeter with an input resistance of ≥10 MΩ (preferably much higher)
d) A calibrated, reversible magnetic field source with a flux density of ≥100 gauss uniform to ±5% over the area of the sample
e) Appropriate electrical switching facilities

Copyright The Institute of Electrical and Electronics Engineers, Inc.
Provided by IHS under license with IEEE
No reproduction or networking permitted without license from IHS Not for Resale

5.2.2 Measurements for determining resistivity, ρ

a) Immerse the sample in LN and wait for temperature equilibration before recording data.
b) Drive current into contact A and out of B while measuring and recording the voltage difference and polarity between C and D.
c) Drive the current into contact B and out of C while measuring and recording the voltage difference and polarity between D and A.
d) Repeat with the current flow reversed and again with the current increased by a factor of 10.

5.2.3 Measurements for determining the hall coefficient, R_H

The procedure for obtaining the data for R_H is similar to the preceding one, but a different sequence of contacts must be used. Also, the data must be obtained with and without a magnetic field applied. The field, when applied, shall be perpendicular to the plane of the sample and should be monitored during the measurements to be sure that the variation is ≤2%. Details for the measurements are as follows:

a) With the magnetic field off, drive current into contact B and out of D while measuring and recording the voltage difference between A and C. This will lead to a computed value of $[R_{BD,AC}]_{B=0}$.
b) Repeat step a) with the magnetic field on. This will lead to a computed value of $[R_{BD,AC}]_{B=B}$.
c) Repeat steps a) and b) with the current flow reversed, and again with the current increased by a factor of 10.

5.2.4 Computation of resistivity, ρ

The resistivity, ρ, can be obtained from equation (1):

$$\rho = 4.53d\left(\frac{R_{AB,CD} + R_{BC,DA}}{2}\right)\cdot f\left(\frac{R_{AB,CD}}{R_{BC,DA}}\right) \quad (1)$$

where

$R_{AB,CD}$ is defined as a fraction in which the numerator is the voltage difference ($V_D - V_C$), and the denominator is the current (in amperes) entering the sample at contact A and leaving through B, with the magnetic field turned off (see figure 5.1).

$f(R_{AB,CD}/R_{BC,DA})$ is a function shown in figure 5.2 for $R_{AB,CD} > R_{BC,DA}$. Invert the argument if $R_{BC,DA} > R_{AB,CD}$.

5.2.5 Computation of the Hall coefficient R_H

The Hall coefficient, R_H, in units of $cm^3\ C^{-1}$, can be obtained from equation (2):

$$R_H = \frac{d}{B}\{[R_{BD,AC}]_{B=B} - [R_{BD,AC}]_{B=0}\} \quad (2)$$

where

$[R_{BD,AC}]_{B=B}$ is the resistivity, $R_{BD,AC}$, in Ω with the magnetic field turned on
$[R_{BD,AC}]_{B=0}$ is the resistivity, $R_{BD,AC}$, in Ω with the magnetic field turned off
B is the magnetic field in units of $V\ s\ cm^{-2}$ ($1\ V\ s\ cm^{-2} = 10^4$ T)
d is the sample thickness in cm

The required polarity of the magnetic field is shown in figure 5.1 a). R_H is positive in p-type material.

Copyright The Institute of Electrical and Electronics Engineers, Inc.
Provided by IHS under license with IEEE
No reproduction or networking permitted without license from IHS
Not for Resale

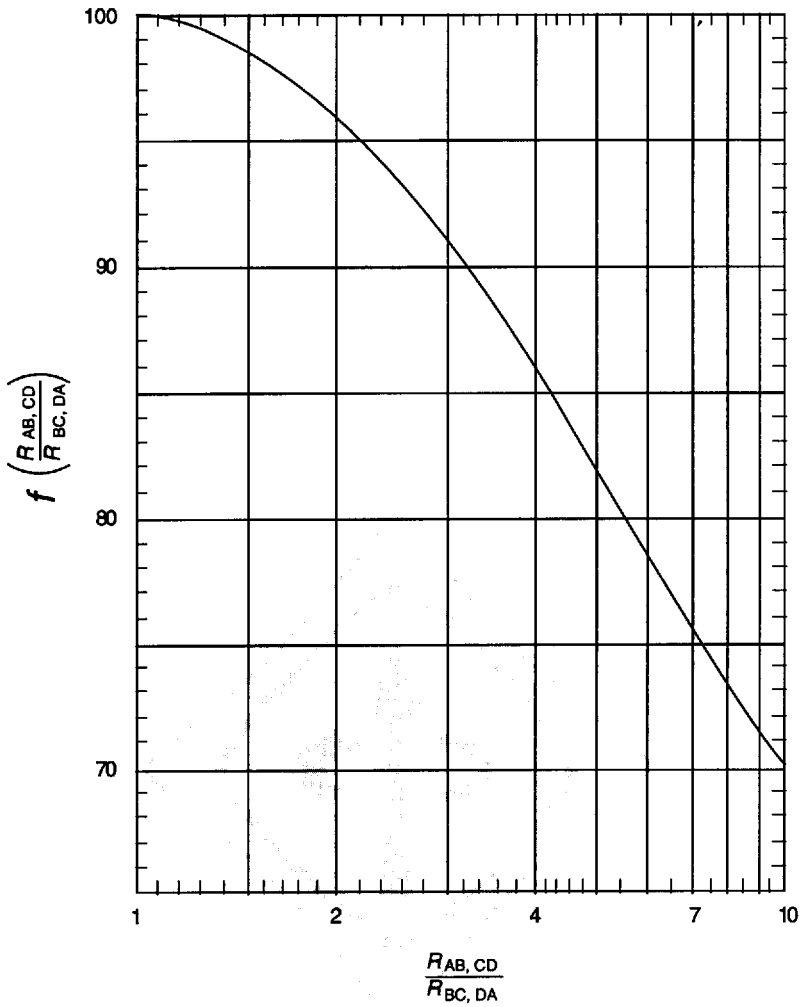


Figure 5.2—$f(R_{AB,CD}/R_{BC,DA})$ vs. $R_{AB,CD}/R_{BC,DA}$

5.2.6 Measurement drift

The quantities $R_{AB,CD}$, $R_{BC,DA}$, and $\Delta R_{BD,AC}$ shall not exhibit a change of more than 5% upon current reversal, magnetic field reversal, or upon changing the current by a factor of 10 (the last artifact may be caused by a voltmeter with insufficiently high input resistance). Also, the preceding quantities shall not exhibit a change of more than 2% over a 5 min period, nor more than 2% during a 5 min interval between measurements. If the preceding conditions are not met, the sample shall be reconditioned (re-etched, new contacts applied) and the measurements shall be repeated.

5.2.7 Active-impurity concentration ($N_A - N_D$) obtained from ρ

The quantity $(N_A - N_D)$ can be obtained from equation (3):

$$N_A - N_D = \frac{1}{\rho e \mu_{(n \text{ or } p)}} \tag{3}$$

Copyright The Institute of Electrical and Electronics Engineers, Inc.
Provided by IHS under license with IEEE
No reproduction or networking permitted without license from IHS

Not for Resale

where

ρ is the resistivity [see equation (1)]
e is the electron charge, $1.6 \cdot 10^{-19}$ C
μ is the drift mobility (see 5.2.7.1) associated with the carrier type of the sample, n or p, according to whether R_H is negative or positive, respectively (see 5.2.8)

If magnetic field reversal and current reversal do not produce a consistent sign for R_H, or if the reversals produce values of $R_{BD,AC}$ that differ by more than 25%, a type shall not be assigned using this technique. If μ, as calculated from 5.2.7.2, is $\leq 10^4$ cm^2 V^{-1} s^{-1}, the sign of the Hall coefficient shall not be used for specifying type.

5.2.7.1 Drift mobility, μ, used in this standard

The values of drift mobility, μ_H, that shall be used in equation (3) are given by equations (4) and (5):

$$\mu_n = 36\,000 \text{ cm}^2\ V^{-1}\ \text{s}^{-1} \tag{4}$$

$$\mu_p = 42\,000 \text{ cm}^2\ V^{-1}\ \text{s}^{-1} \tag{5}$$

The preceding drift mobilities for HPGe at 77 K are not universally agreed upon. Those given here represent conservative choices to avoid understatement of $|N_A - N_D|$.

5.2.7.2 Drift mobility from a van der Pauw measurement

The data necessary to calculate μ independently for each sample can be obtained from a van der Pauw measurement. The Hall mobility is defined by equation (6):

$$\mu_H = \frac{|R_H|}{\rho} \tag{6}$$

where

$|R_H|$ is the absolute value of the Hall coefficient in cm^3 C^{-1}
ρ is the resistivity [see equation (1)]

and is related to the drift mobility, μ, by equation (7):

$$\mu = \frac{\mu_H}{r} \tag{7}$$

where

μ_H is obtained from equation (6)
r is a constant near unity (see 5.2.8, 5.2.8.1, and 5.2.8.2)

Values of μ obtained from van der Pauw data may be lower than true bulk values for several reasons:

a) Poor contacts
b) The effects of surface charge
c) Macroscopic nonuniformity
d) Microscopic inhomogeneities

Copyright The Institute of Electrical and Electronics Engineers, Inc.
Provided by IHS under license with IEEE
No reproduction or networking permitted without license from IHS
Not for Resale

The low mobility caused by item d) results from local shallow fluctuations in potential that impede carrier flow at electric fields of $<1V\ cm^{-1}$. Neutral impurity scattering also may reduce mobility, but this is an unusual problem in HPGe.

The low mobilities do not forecast lower carrier velocity at the high fields used in detector operation ($\approx$1 kV cm^{-1}), but they do present practical problems in determining $|N_A - N_D|$. Although this standard is restricted to material with $\mu > 25\ 000\ cm^2\ V^{-1}\ s^{-1}$ at 77 K (see 5.3.1.2), it should not be inferred that material with lower μ is unsuitable for nuclear detectors. It is only that, for such material, determination of $|N_A - N_D|$ must proceed along lines different from those specified here.

NOTE—Low values of mobility that persist through repeated etching and contacting of the sample may be taken as an indication of sample inhomogeneity.

5.2.8 Active-impurity concentration $|N_A - N_D|$ obtained from R_H

The quantity $|N_A - N_D|$ can be obtained from equation (8):

$$N_A - N_D = \frac{r}{eR_H} \tag{8}$$

where

r is a constant between near unity (see next paragraph and 5.2.8.1 and 5.2.8.2)
e is the electron charge, $1.6 \cdot 10^{-19}$ C
R_H is the Hall coefficient

In the classical high-field limit, $r = 1$ and the carrier completes many cyclotron orbits before a scattering event. Unfortunately, for germanium at 77 K, this limit can be achieved only at magnetic field strengths beyond those conveniently available: $B \geq 10$ T. At lower fields strengths, $r = \langle \tau_r^2 \rangle / \langle \tau_r \rangle^2$ for an ideal semiconductor, where τ_r is the relaxation time of a carrier and $\langle\ \rangle$ indicates averaging over occupied states. In HPGe, τ_r depends on the details of the band structure of the carrier and on the scattering mechanisms. Also, r is different for n-type and p-type HPGe (see the next two subclauses).

5.2.8.1 Factor r in n-type HPGe

In n-type HPGe at 77 K, r approaches 0.83 as B approaches zero for all magnetic field orientations (see [B17]). For finite B, r depends both on the direction of the B vector and the induced Hall electric field vector with respect to the crystallographic axes. This dependence is due to the strong anisotropy of the ellipsoidal constant-energy surfaces in the conduction band of germanium. For $B < 0.1$ T, r may be taken as 0.83. For $B > 0.1$ T, r must be corrected for magnetic field strength, taking into account the crystallographic orientation of the sample. This correction is given in figure 5.3 for two orientations of the magnetic field, B, and current, I (see [B17]).

5.2.8.2 Factor r in p-type HPGe

Because constant-energy surfaces in the valence bands are much less anisotropic than in the conduction band, the dependence of r on the orientation is small enough to be neglected in p-type germanium. A more significant effect results from the degeneracy of the fast-hole and slow-hole bands at low energies. The effect of the fast holes, approximately 4.5% of the hole concentration, is to raise r substantially at low fields (see [B5] and A.5.2.8.2).

The factor r for p-type HPGe is plotted as a function of magnetic field strength in figure 5.4. (This graph was generated for this standard by measuring R_H as a function of B up to 0.4 T for several HPGe samples exhibiting differing R_H values. At 0.4 T, a value of $r = 1.03$ was assumed.)

Copyright The Institute of Electrical and Electronics Engineers, Inc.
Provided by IHS under license with IEEE
No reproduction or networking permitted without license from IHS Not for Resale

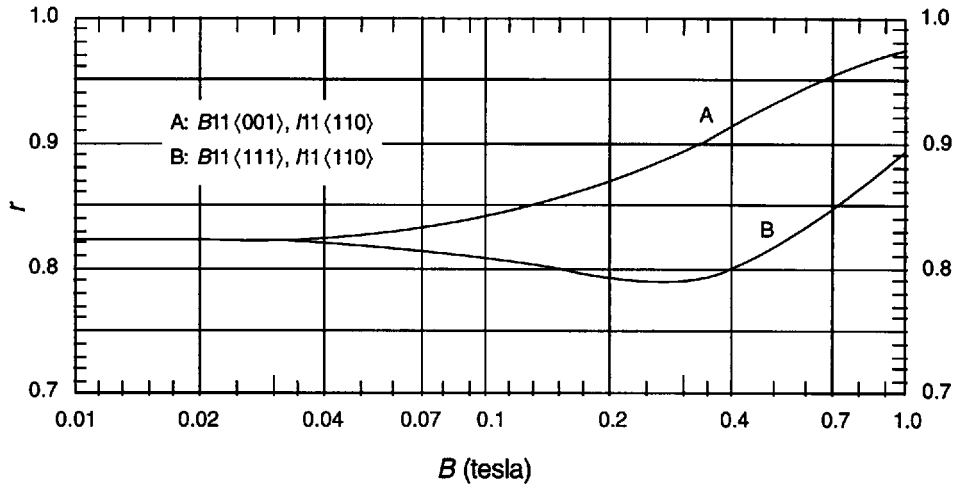


Figure 5.3—Factor *r* for n-type HPGe, two crystallographic orientations

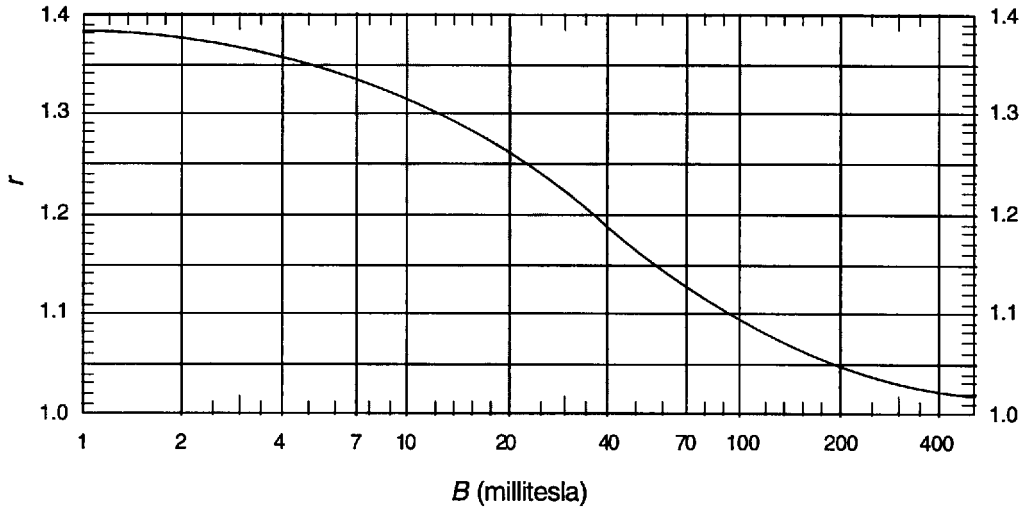


Figure 5.4—Factor *r* for p-type HPGe

5.3 Spatial dependence of ($N_A - N_D$)

If the volume of an HPGe detector is much greater than the volume of the van der Pauw sample (as is usually the case), it is important to determine the axial and radial variations of ($N_A - N_D$). Nonplanar growth interfaces, radial irregularities in microscopic growth speed, and diffusion from or toward the surface may cause a radial gradient $\Delta(N_A - N_D)$. Axial variations are caused by the nonunity distribution coefficients of the residual impurities (see [B23]). There also are inhomogeneities over tens to hundreds of micrometers due to the microscopic growth-rate dependence of the effective distribution coefficient. These inhomogeneities or striations are correlated with the rotation rate of the ingot during crystal growth or are induced by thermal fluctuations during the growth period. The inhomogeneities may cause low measured mobilities near p–n transitions in compensated samples.

Copyright The Institute of Electrical and Electronics Engineers, Inc.
Provided by IHS under license with IEEE
No reproduction or networking permitted without license from IHS

Not for Resale

5.3.1 Radial variations in ($N_A - N_D$)

For the analysis presented here, it is assumed that ($N_A - N_D$) is a linear function of radius, and that the average $\langle N_A - N_D \rangle$ of interest is the arithmetic mean of the measurements made at the center and edge of a whole slice. The radial variation $\Delta(N_A - N_D)_{rad}$ in a slice is defined in equation (9):

$$\Delta(N_A - N_D)_{rad} = (N_A - N_D)_{edge} - (N_A - N_D)_{center} \tag{9}$$

The following three techniques are acceptable for determining the radial variations.

5.3.1.1 Effective mobility technique

In a measurement of a whole slice, if μ is within 10% of the theoretical values given by equations (4) or (5), the measured value of ($N_A - N_D$) may be considered to be the true value, and the variation in ($N_A - N_D$) may be assumed to be less than 15%.

5.3.1.2 Cloverleaf technique

This method may be used if the van der Pauw measurement on a whole slice produces a value of μ >30 000 $cm^2\ V^{-1}s^{-1}$ (see 5.2.7.2). The slice may then be machined or cut to produce notches between the contacts extending inward by at least half the radius of the slice. The slice shall then be re-etched and remeasured. In the new geometry, only the central area contributes significantly to the measurement. In this instance, if $\mu_{cloverleaf} > 25\,000\ cm^2\ V^{-1}\ s^{-1}$, equations (10) and (11) apply:

$$\langle N_A - N_D \rangle = (N_A - N_D)_{slice} \tag{10}$$

$$\Delta (N_A - N_D)_{rad} = 2 [(N_A - N_D)_{slice} - (N_A - N_D)_{cloverleaf}] \tag{11}$$

5.3.1.3 Dice technique

A slice also may be analyzed by taking small disks or squares from the edge and center. The maximum lateral dimension of those pieces shall be less than 1/4th the diameter of the slice. The edge sample should be within 1 mm of the periphery. In this case, if $\mu > 25\,000\ cm^2\ V^{-1}\ s^{-1}$ in each measurement, then equation (12) applies:

$$\langle N_A - N_D \rangle = \frac{(N_A - N_D)_{edge} + (N_A - N_D)_{center}}{2} \tag{12}$$

and $\Delta|N_A - N_D|_{rad}$ is given by equation (9). Note that the radial variation is positive for acceptor concentration *increasing*, or donor concentration *decreasing*, outward along a radius.

5.3.2 Axial variations in ($N_A - N_D$)

Axial variations are obtained by measuring ($N_A - N_D$) on slices at different axial locations.

5.3.3 Measurements on slices intended for detector fabrication

With a slice intended for a planar detector (diameter » length), ($N_A - N_D$) is obtained from whole-slice measurements.

With a piece intended for a coaxial detector (diameter ≈ length), measurements of ($N_A - N_D$) and $\Delta(N_A - N_D)$ shall be made on slices adjacent to each end of the piece. However, for a section of an as-grown

Copyright The Institute of Electrical and Electronics Engineers, Inc.
Provided by IHS under license with IEEE
No reproduction or networking permitted without license from IHS Not for Resale

crystal that is large enough to produce several coaxial detectors, it may be uneconomic to slice the crystal at several points along the axis for the purpose of characterization. In this instance, interpolation is required from measurements made on slices at the two ends. Because there are various ways of doing this and because it may be necessary to rely on supplementary methods of measurement, the procedure to be followed should be agreed upon between the crystal producer and the detector manufacturer.

6. Deep-level transient spectroscopy (DLTS) for the characterization of point-defect trapping centers (N_T)

When HPGe is fabricated into a nuclear radiation detector, electrically active defects may occur with levels deep enough to prevent trapped carriers from being re-emitted in a time short compared with the shaping time of the linear amplifier. The effect may cause peak broadening and tailing to occur in recorded spectra. In this standard, a deep level is one that is considered to have an emission rate of $<10^6$ s^{-1} at 77 K. Capacitance-transient measuring techniques, particularly DLTS (see [B15]), have proved useful in identifying and quantifying several harmful deep acceptor levels.

In DLTS, the diode is held at a quiescent reverse-bias voltage, V_r. At that voltage, the diode will exhibit a capacitance, C_f. Then, a voltage pulse, V_p, is applied that reduces the bias, thereby introducing majority carriers into a region that was previously depleted. At the end of the pulse (when the voltage returns to V_r), the majority carrier levels that were filled cause the diode to exhibit a capacitance, C_i; but those levels immediately begin emptying, and the capacitance returns exponentially to its original value, C_f.

In Lang's method (see [B15]), this change is analyzed with a double boxcar averager that produces a signal proportional to $C(t_2) - C(t_1)$, which is the change in capacitance C occurring between t_1 and t_2. The gating waveforms and C vs. time are shown in figure 6.1.

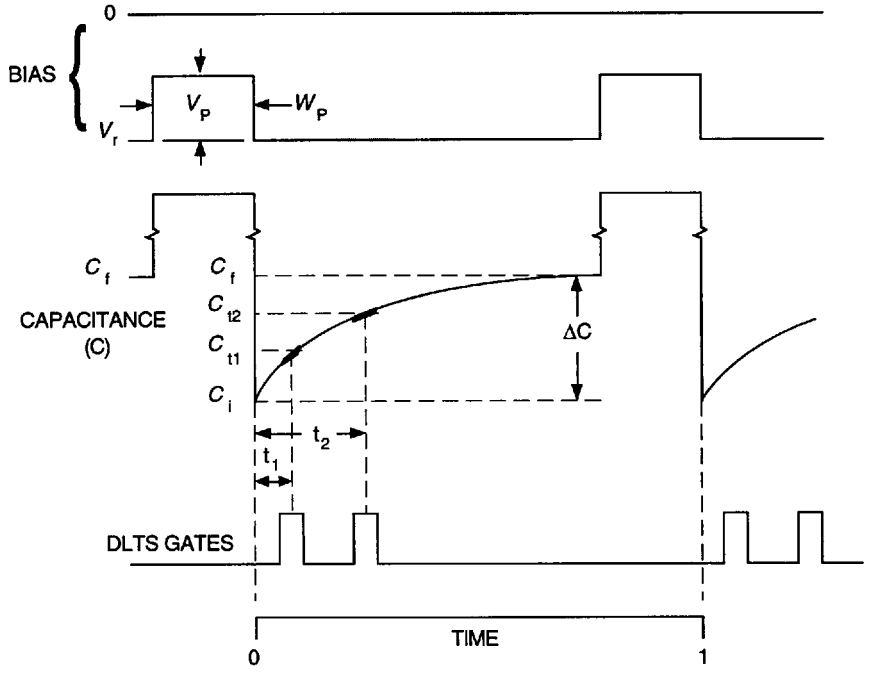


Figure 6.1—DLTS waveforms and gate timing

Copyright The Institute of Electrical and Electronics Engineers, Inc.
Provided by IHS under license with IEEE
No reproduction or networking permitted without license from IHS
Not for Resale

In DLTS, $C(t_2) - C(t_1)$ is plotted versus temperature. This capacitance difference depends on the carrier emission rate, e_r, which increases strongly with temperature. The DLTS signal from a particular level is a maximum at a unique temperature (see 6.3.1) for which the emission time, $\tau = e_r^{-1}$, meets the condition of equation (13) (see [B15]):

$$\tau_{max} = \frac{(t_2 - t_1)}{\ln\left(\frac{t_2}{t_1}\right)} \tag{13}$$

where t_2 and t_1 refer to the times shown in figure 6.1.

There is a difficulty with DLTS of HPGe. At low values of $|N_A - N_D|$, the resistance of undepleted germanium may be not only high, but may also be a strongly increasing function of temperature over the range of interest: 15 K to 220 K.

Depending on $(N_A - N_D)$, sample thickness, bias, frequency of the capacitance-measuring circuit, and temperature, the resistance may be comparable to the capacitive reactance, particularly above 100 K. The preceding affects spectrometer sensitivity and the reliability of peak identification. Corrections for equivalent circuit effects are presented in 6.3.4.

Occasionally, extended defects are also observed in DLTS of HPGe (see [B24] and [B16]), but quantitative interpretation of the data is unclear. For this reason, the characterization of extended defects by DLTS is not included in this standard.

The examination of minority-carrier deep levels requires the injection of minority carriers. Since saturation of these is difficult to obtain and demonstrate, the method is more qualitative than quantitative. Such tests will not be dealt with in this standard.

6.1 Equipment

The measurements described here are based on the boxcar integrator method of Lang (see [B15]); however, several other valid and acceptable instrumentation schemes may be used.

For the Lang method, the required equipment includes

a) A capacitance meter capable of measuring 1 to 100 pF full scale ± 2%. A three-terminal instrument is required so that the effects of stray capacitance from the sample contacts to the surroundings are eliminated. The instrument must allow the application to the sample of a sustained dc bias of at least 10 V, and the instrument must respond with a rise time much less than the smallest emission time constant to be measured. Also, a means of limiting the large transient during the filling pulse, V_p, may be required.

   A capacitance bridge is not recommended because its response time is slow and because its signal-to-noise ratio is inferior to that of the capacitance meter.

b) A pulse generator capable of changing the bias voltage from one level to a different one, with a switching time that is much less than the smallest emission time-constant to be measured. It may be necessary to connect an additional voltage source in series with the pulse generator in order to extend the range of reverse bias.

c) A double boxcar integrator (or equivalent) with adjustable gate duration, two separately controllable gate delay times, and adjustable sampling time.

d) A recording system capable of digitally or continuously measuring the difference in capacitance between the two gate delay times as a function of temperature.

Copyright The Institute of Electrical and Electronics Engineers, Inc.
Provided by IHS under license with IEEE
No reproduction or networking permitted without license from IHS Not for Resale

e) An oscilloscope that allows measurement of the gate delay times and observation of the capacitance transient.
f) A cryostat in which the sample temperature can be varied between 15 K and 220 K.
g) A thermometry system that allows measurements of sample temperature to ±0.5 K while the temperature is varying.

6.2 Sample selection and preparation for DLTS

The size of the sample and its location in the as-grown crystal are critically important because deep-level concentrations may have strong radial and axial gradients (see [B16]). For DLTS characterization of an HPGe crystal that is to be made into a coaxial detector, the following selection procedure is specified: for p-type, a sample shall be taken from a slice adjacent to the seed end; for n-type, a sample shall be taken from a slice adjacent to the tail end. The sample shall be located midway between the "flats" formed during crystal growth, and its edge shall be within 2 mm of the slice's perimeter. If the sample is square, it should be ~6 mm on a side. If the sample is a disc, the diameter should be ~6 mm.

6.2.1 Junction preparation

To determine the free-carrier type and concentration $|N_A - N_D|$, van der Pauw measurements shall be made (see clause 5) prior to junction formation in the sample.

The junction may be formed by any technique that provides rectification: diffusion, implantation, or metallization. To prevent diffusion of Cu-related centers into the sample, processing temperatures shall be kept below 550 K and the thermal processing time shall be less than 2 h if pacification techniques are not used. Uncontacted surfaces shall be etched immediately before measurement as a precaution against unwanted surface effects.

6.3 Measurement procedure

6.3.1 DLTS signal vs. temperature

The temperature of the sample shall be varied at a rate of <0.1 K s^{-1} while recording the DLTS signal. The results shall be graphed. To obtain the level parameters K_n and ΔE_n in table 1, several DLTS temperature scans are required in which the gate separation time, $t_2 - t_1$, is varied while the ratio of t_2/t_1 is held constant. Typically, $t_2 - t_1$ is between 500 µs and 10 ms while the ratio t_2/t_1 is ≈5.

6.3.2 (Capacitance)$^{-2}$ vs. voltage

The temperature shall be stabilized below the lowest-temperature DLTS peak appearing in the spectrum ($10\ K \le T \le 20\ K$) to ensure freeze-out of all deep-level carriers. It shall be verified that the sample is undepleted at V_r. For an abrupt junction with flat-band surfaces, a least-squares fit of C^{-2} vs. V should approximate a straight line with a slope, m, which may then be used to estimate the concentration $|N_A - N_D|$ from equation (14):

$$|N_A - N_D| = \frac{8.86 \cdot 10^6}{A^2 m} \tag{14}$$

where

$|N_A - N_D|$ is in units of cm^{-3}
A is the diode area in cm^2
m is the slope of the C^{-2} vs. V plot $[(pF)^{-2}\ V^{-1}]$

Copyright The Institute of Electrical and Electronics Engineers, Inc.
Provided by IHS under license with IEEE
No reproduction or networking permitted without license from IHS
Not for Resale

The commonly used rectifying contact for p-type HPGe is made by a lithium diffusion, resulting in a poor approximation to an abrupt junction. Surface charge also contributes distortion, as do stray capacitances, nonuniform impurity distributions, and other effects. The use of equation (14) assumes that the space charge region terminates abruptly. This will not be true if deep levels are present and may not be justified in extremely pure materials at higher temperatures. Because of these difficulties, the C^{-2} vs. V curve shall be used only to check the qualitative behavior of the diode. The concentration of shallow levels shall be obtained from a van der Pauw measurement (see 5.2.7). To meet the conditions of this standard, the concentration obtained from equation (15) (by taking the C^{-2} vs. V slope at V_r) shall be within 20% of that deduced from the van der Pauw measurement. Corrections must be made for the concentration of levels that are ionized in thermal equilibrium at the temperature of that measurement, but which are frozen out during the lower-temperature C^{-2} vs. V measurement.

6.3.3 Corrections for equivalent-circuit effects

A simplified equivalent circuit that is appropriate for DLTS measurements of HPGe samples (see [B21] and [B6]) consists of three components that can be ascribed to the depleted and undepleted regions of the sample:

a) C_d is the capacitance across the depleted region.
b) R_p is the leakage resistance in parallel with the depleted region.
c) R_s is the series resistance of the sample, which includes the resistance of the undepleted region and the resistance of the contacts.

The first of these, C_d, is the component of interest in DLTS measurements. It depends on the applied voltage, $|N_A - N_D|$ in the depletion region, and the area of the contacts.

The second component, R_p, usually is so high in good material operating at cryogenic temperatures that its effect can be neglected.

The last component, R_s, frequently affects the determination of C_d. If R_s is due predominantly to the contacts, then reworking them may reduce the resistance to a level not requiring corrections. If R_s is due predominantly to the resistance of the undepleted region of the diode, it often is possible to test the sample in a temperature range where R_s is too low to require corrections. Corrections are discussed further in the next section for situations where they cannot be avoided.

6.3.3.1 Capacitance meter

Capacitance meters used in the semiconductor industry are three-terminal devices — the samples are connected to the meter through shielded cables. The shields act as guard electrodes to prevent the desired depletion-region capacitance from being affected by the capacitance from the sample contacts to the surroundings. Capacitance can be read directly from a panel-mounted voltmeter, and there is an output connector that allows the capacitance signal V_c to be observed on an oscilloscope. The operating frequency, f (≈1 MHz), is chosen by the manufacturer of the meter to give a good signal-to-noise ratio. That frequency also has the attribute of making the series time constant of the sample $\ll 1/2\pi f$ and the parallel time constant $\gg 1/2\pi f$.

The meter sees the equivalent of a capacitance and resistance in parallel (see [B21]) across its input terminals. Because the true circuit is more appropriately a capacitance and resistance in series, it was suggested (see [B21]) that equation (15) can be used to compute the series capacitance from the measured parallel capacitance:

$$C_d = C_m (1 + D_s^2) \tag{15}$$

Copyright The Institute of Electrical and Electronics Engineers, Inc.
Provided by IHS under license with IEEE
No reproduction or networking permitted without license from IHS Not for Resale

where

C_d is the capacitance of the depleted region
C_m is the measured parallel equivalent capacitance
D_s is the series-circuit dissipation factor $\omega R_s C_d$ (D_s is referred to as Q in [B21], but the generally accepted meaning of Q for a series circuit is $1/\omega R_s C_d$, or D_s^{-1})

To determine the value of D_s at a particular operating temperature, a temperature plot of C vs. T should be made on the sample. A plateau can be expected somewhere in the range of 20 K to 100 K, indicating that D_s has been reduced to «1 and that $C_m = C_d$. If the DLTS peak falls on the plateau, no corrections are necessary; but, if it is off the plateau on the high temperature side, C_m will decrease. D_s can then be inferred from equation (15). This scheme assumes that the contact resistance is low compared with the resistance of the undepleted region of the diode and that the change in capacitance due to the emptying of deep levels is small compared with the correction term in equation (15).

In DLTS measurements involving capacitance changes, the relative change in series capacitance can be obtained from the measured relative change in parallel capacitance by applying the correction (see [B21] and [B6]) given in equation (16). This correction is valid for the small signal case, $\Delta C_d < 0.2\ C_d$.

$$\frac{\Delta C_d}{C_d} = \frac{\Delta C_m}{C_m} \exp\left[\frac{1 + D_s^2}{1 - D_s^2}\right] \tag{16}$$

where

$\Delta C_d/C_d$ represents the corrected fractional change in capacitance of the depleted region
D_s is the dissipation factor, $\omega R_s C_d$
$\Delta C_m/C_m$ is the measured fractional change in capacitance

Note the singularity in equation (16) when $D_s = 1$. The equation should not be used if $D_s > 0.8$. If $D_s < 0.2$, the correction is unnecessary.

6.3.4 Corrections for high trap concentrations and for voltage pulse height

The calculated deep-level concentration, N_T, shall also be corrected for high trap concentrations and for the height of the voltage pulse. Equation (17) takes both of these effects into consideration (see [B21]). An alternate method is given in 6.3.5.

$$N_T = N_B \frac{\Delta C_d}{C_d} \frac{2 - \dfrac{\Delta C_d}{C_d}}{\left(1 - \dfrac{\Delta C_d}{C_d}\right)^2} \frac{V_r + V_{bi}}{\Delta V_p} \tag{17}$$

where

N_B is the net concentration of all shallower levels derived from a van der Pauw measurement at 77 K and DLTS analysis
V_{bi} is the built-in potential of the diode (a value of 0.5 V may be assumed)
V_r is the bias voltage (see figure 6.1)
V_p is the pulse height (see figure 6.1)

Copyright The Institute of Electrical and Electronics Engineers, Inc.
Provided by IHS under license with IEEE
No reproduction or networking permitted without license from IHS
Not for Resale

It may be assumed that the Cu-H_x (0/-) level and all shallower levels are ionized when thermal equilibrium is established at 77 K, where the notation 0/- refers to the believed charged states, neutral before hole emission and singly-ionized after, and the subscript of H refers to unknown stoichiometry.

6.3.5 $\Delta V_c / V_p$ technique for measuring N_T

An alternative technique[4] is available for determining the level concentration, N_T. It is implemented in conjunction with, and immediately following, identification by DLTS; and it has the merits that overt capacitance measurements are not required (although the capacitance meter must remain part of the setup). Also, no corrections are needed for high trap concentrations, series-resistance effects, or filling-pulse height, and inaccuracy of the capacitance meter does not affect the result. The procedure is as follows:

a) With the oscilloscope connected to the output of the capacitance meter, obtain an entire capacitance transient waveform on the oscilloscope screen as described early in clause 6. The exponentially increasing portion of the waveform should resemble the upper one in figure 6.2.

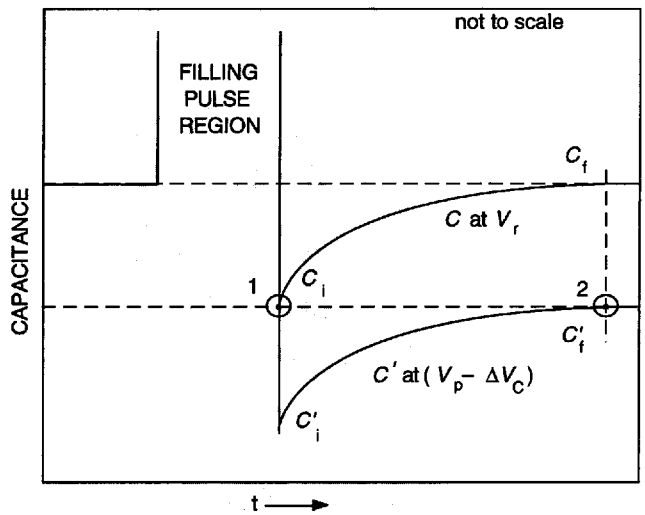


Figure 6.2—$\Delta V_c / V_p$ waveforms

b) Record the height of the filling pulse, V_p.

c) Note the vertical position of the encircled point 1, which corresponds to the initial capacitance, C_i.

d) Increase the reverse bias, V_r, by an amount, V_c, such that the signal corresponding to the final capacitance, C'_f, at the encircled point 2 is at the same vertical level as point 1; and record the ΔV_c necessary to establish this condition. Care must be taken to ensure that the bias does not completely deplete the diode at C_i or C'_i. If that occurs, a smaller initial bias voltage, V_r, shall be chosen.

e) N_T may then be computed from equation (18):

$$N_T = \frac{\Delta V_c}{V_p} N_B \qquad (18)$$

[4]L. S. Darken, not previously published.

Copyright The Institute of Electrical and Electronics Engineers, Inc.
Provided by IHS under license with IEEE
No reproduction or networking permitted without license from IHS
Not for Resale

6.4 Majority-carrier deep levels in p-type HPGe

Majority deep levels that have been reported in p-type HPGe are listed in table 1 with the identifications suggested by the authors.

Table 1—Majority-carrier deep levels in p-type HPGe

$$e_r = K_n T^2 \exp(-\Delta E_n / kT)^*$$

Impurity center†	Ionization level‡	K_n kelvins^{-2} s^{-1}	ΔE_n eV	Reference
Cu_s	0/-	6.0	0.037	[B23]
Cu-H	0/-	8.6	0.062	[B23]
G	?	[τ = 6.1 ms at 70 K]		[B15]
Cu-H-Li	?	21.8	0.160	[B23]
Cu-H	-/- -	4.5	0.185	[B23]
Cu_s	-/- -	146	0.322	[B23]

*In this equation, e_r is the emission rate, K_n and ΔE_n are parameters of the level n, k is Boltzman's constant, and T is temperature in kelvins.
†Cu_s refers to substitutional copper.
‡0/- refers to (neutral)/(singly ionized) *before/after* hole emission.
-/- - refers to (singly)/(doubly ionized) *before/after* hole emission.

Because the capture cross-sections of the defects differ, the concentration of each defect (or the upper bound on the concentration) shall be reported.

The first ionization levels of Cu and Cu-H_x are listed, but are not considered trapping levels for the purposes of this standard. If interferences do not exist, these ionization levels should be used to determine the concentration of the center.

Deep levels observed but not listed in table 1 may be identified by the parameters K_n and ΔE_n or, more simply, by the emission rate at a particular temperature (see the equation for e_r at the top of the table). It should be verified that previously unpublished defect levels really are bulk effects, rather than surface effects or contact-related phenomena, by measuring the magnitude of the DLTS signal as a function of pulse height, V_p, at the same V_r. For a uniformly distributed bulk defect, there is a linear relationship between the magnitude of the DLTS signal and V_p. It shall be verified that the emission from the level is exponential (see [B24] and [B16]). It also shall be verified that capture by such a level is exponential. This shall be done by observing the strength of the DLTS signal or ΔC vs. W_p, where W_p is the duration of the filling pulse. For an isolated defect level, there exists a τ_c such that signal strength complies with equation (19):

$$\frac{[\Delta C_d]_{(W_p = \infty)} - [\Delta C_d]_{(W_p)}}{[\Delta C_d]_{(W_p = \infty)}} = \exp\left(\frac{-W_p}{\tau_c}\right) \quad (19)$$

Copyright The Institute of Electrical and Electronics Engineers, Inc.
Provided by IHS under license with IEEE
No reproduction or networking permitted without license from IHS
Not for Resale

6.5 Majority-carrier deep levels in n-type HPGe

Majority-carrier deep levels reported in n-type high-purity germanium exhibited broader peaks than expected for single isolated-defect levels (see [B12]). In some cases, capture kinetics similar to those observed in plastically deformed samples were reported (see [B22]). As indicated in clause 6, this standard does not address DLTS of extended defects. Isolated-defect trapping levels shall be characterized and reported in the same manner as in p-type material. Also, both exponential emission from and exponential capture by such levels shall be demonstrated.

6.6 Reporting

If the measurement technique is different from that of Lang (see [B15]), the results shall be preceded by a description of the technique that was used or by a literature citation to such a description. In all cases, the operating frequency of the capacitance bridge or meter shall be stated. If the Lang method is used, the value of τ_{max} shall be stated as well. Observed levels that can be quantified under the rules given in this standard shall be tabulated with their concentrations. Upper limits on the concentration at the centers listed in table 1 that are not observed may be deduced from the minimal detectable capacitance transient at the appropriate temperature. If a DLTS peak is observed but cannot be quantified (e.g., because of high D_s), the reason shall be stated.

7. Crystallographic properties

There have been many reports concerning the effects of crystallographic defects on detector performance. It is noteworthy that absolute crystalline perfection usually is undesirable because as-grown dislocation-free germanium contains an unacceptably high concentration of electrically active vacancy-related point defects (see [B11]). However, dislocations themselves may possess electrical activity due to any of several mechanisms (which of those are important is presently unclear). The effect of dislocations on charge collection has received attention (see [B8], [B11], [B13], [B14], and [B26]). In one study, the DLTS peaks could be related to the type of dislocation (see [B26]). For adequate charge collection in particular detector geometries, [B8] and [B26] cite upper limits on etch-pit density. However, since the type of dislocation and its electrical activity appear to depend strongly on growth conditions (see [B14] and [B13]), these limits cannot be assumed to be universally applicable. Complete crystallographic information is never available; and if it were, the state of the knowledge in this field is such that device properties could not be predicted from these data. However, there is legitimate interest from the device standpoint in some general crystallographic properties as discussed below. For example, aside from dislocations, certain types of large-scale crystallographic defects (twin planes, grain boundaries, and some lineage) frequently generate excess leakage current.

7.1 Crystallographic orientation

Crystalline germanium has a diamond structure, and the crystallographic orientation is referred to the conventional unit cube. Electronic-transport, mechanical, and etching characteristics are generally anisotropic. The crystallographic orientation should be determined either optically or by x-ray diffraction. Useful guidance in using those techniques is found in Section 2 of [B1], which contains semiconductor single-crystal descriptions of both optical and x-ray diffraction orientation. It is accepted practice to assume the axial orientation of the crystal from the previously measured axial orientation of the seed, providing that no twins or grain boundaries are present in the crystal.

7.2 Sample preparation

The as-grown ingot should be visually examined in strong light for twin planes or grain boundaries. Sections of the crystal that display either feature are not considered to be monocrystalline. Slices for etch-pit evalua-

Copyright The Institute of Electrical and Electronics Engineers, Inc.
Provided by IHS under license with IEEE
No reproduction or networking permitted without license from IHS Not for Resale

tion shall all be cut adjacent to the tail end of the piece being characterized and normal to the growth direction, unless other positions are specified in the producer-user relationship.

7.2.1 Preferential etching

Crystallographic perfection is most conveniently assessed by preferential etching techniques that produce pits at the intersection of a dislocation with the surface being etched. The procedure consists of

a) Mechanical preparation
b) Polish etching
c) Preferential etching
d) Examination under an optical microscope
e) Tabulation of results

Characteristics and limitations of this technique are discussed in Section 2 of [B3].

7.2.2 Etching methods

Polish etching shall be performed using one of the etching techniques described in 5.1.3. The chemically polished slice shall then be immersed in a preferential etch long enough to develop dislocation etch pits, usually about 90 s. Dislocation etch pits are characterized by pointed bottoms. The following preferential etches shall be used:

a) *Dislocation etch (111):* Dissolve 8 g $AgNO_3$ in 160 ml water, then add 80 ml HNO_3 (70% by weight) and 160 ml HF (49% by weight). Do not use until 15 min after mixing. Discard after 4 h.
b) *Dislocation etch (100):* Dissolve 25 g $Cu(NO_3)_2 \cdot 3H_2O$ in 500 ml water, then add 250 ml HNO_3 (70% by weight) and 500 ml HF (49% by weight). Store in polyethylene or polypropylene bottle.
c) *Dislocation etch (110):* Dissolve 12 g (KOH) and 8 g $K_3Fe(CN)_6$ in 100 ml water. Discard after 4 h.

> ***Caution:*** *The preceding etchants deposit metallic ions. If not removed, they may have an adverse effect on a device made from the material.*

7.2.3 Etch-pit density

It is recognized that the etch-pit distribution may be nonuniform; therefore, no procedure is prescribed for selecting the regions to be counted. It is recommended, however, that dislocations be counted in at least three different 1 mm × 1 mm areas located at the center, edge, and a radially-intermediate location on the slice. If this is done, at least 150 etch pits shall be counted per slice, if this many exist.

7.2.4 Lineage

Dislocation etch pits sometimes are organized into lines representing small-angle grain boundaries in the crystal. Those patterns are called "lineage" and can be characterized by the spacing between dislocation etch pits and the total length of the structure, measured in terms of the slice radius. By definition, the etch-pit spacing for lineage must be <40 μm.

7.2.5 Mosaic

A mosaic is a curled lineage structure with line-spacing greater than one per millimeter.

Copyright The Institute of Electrical and Electronics Engineers, Inc.
Provided by IHS under license with IEEE
No reproduction or networking permitted without license from IHS
Not for Resale

7.3 Reporting

A statement characterizing the crystallography of a piece of HPGe shall include:

a) The axial orientation of the piece. This is also the orientation of the slice used for the evaluation of dislocations unless otherwise stipulated.
b) A statement indicating whether the piece is monocrystalline (no twin planes or grain boundaries) or polycrystalline.
c) The presence of lineage, regions of etch-pit density greater than four times average, dislocation-free areas larger than 2 mm in diameter, and mosaic structures.
d) The average etch pit density and the total number of etch pits counted.

8. Bibliography

[B1] ASTM F26-84, Standard Method for Determining the Orientation of a Semiconductive Single Crystal.

[B2] ASTM F76-84, Standard Method for Measuring Hall Mobility and Hall Coefficient in Extrinsic Semiconductor Single Crystals.

[B3] ASTM F389-84, Standard Test Method for Crystallographic Perfection of Germanium by Preferential Etch Techniques.

[B4] ASTM F978-86, Standard Test Method for characterizing Semiconductor Deep Levels by Transient Capacitance Techniques.

[B5] Beer, A. C. and Williardson, R. K., *Phys. Rev.*, vol. 110, pp. 1286, 1958.

[B6] Broniatowski, A. and Bourgoin, J., *Phys. Rev. Lett.*, vol. 48, pp. 424, 1982.

[B7] Darken, L. S., *Materials Research Society Symposium Proceedings,* vol. 16, pp. 47, 1983.

[B8] Glasow, P. A. and Haller, E. E., *IEEE Transactions on Nuclear Science*, vol. NS-23, no. 1, pp. 92, 1976.

[B9] Hall, R. N., *IEEE Transactions on Nuclear Science*, vol. NS-21, no. 1, pp. 260, 1974.

[B10] Haller, E. E., Hansen, W. L., and Goulding, F. S., *Advances in Physics*, vol. 30, pp. 93, 1981.

[B11] Haller, E. E., Hubbard, G. S., Hansen, W. L., and Seeger, A., *Inst. Phys. Conf.*, ser. 31, pp. 309, 1977.

[B12] Haller, E. E., Li, P. P., Hubbard, G. S., and Hansen, W. L., *IEEE Transactions on Nuclear Science*, vol. NS-26, no. 1, pp. 265, 1979.

[B13] Hubbard, G. S. and Haller, E. E., *J. Electron. Mater.*, vol. 9, pp. 51, 1980.

[B14] Hubbard, G. S., Haller, E. E., and Hansen, W. L., *IEEE Transactions on Nuclear Science*, vol. NS-26, no. 1, pp. 303, 1979.

[B15] Lang, D. V., *J. Appl. Phys.*, vol. 45, pp. 3022, 1974.

[B16] Manglesdorf, P. C., Jr., *J. Appl. Phys.*, vol. 30, pp. 442, 1959.

[B17] Miyazawa, H. and Maeda, H., *J. Phys. Soc. Japan*, vol. 15, pp. 1924, 1960.

Copyright The Institute of Electrical and Electronics Engineers, Inc.
Provided by IHS under license with IEEE
No reproduction or networking permitted without license from IHS

Not for Resale

[B18] Restelli, A., *Semiconductor Detectors*. A. Bertolini and A. Coche, Ed., New York: Wiley Interscience, 1968.

[B19] Simoen, E., Clauws, P., Broeckx, J., Vennik, J., van Sande, M., and De Laet, L., *IEEE Transactions on Nuclear Science*, vol. NS-29, no. 1, pp. 789, 1982.

[B20] Simoen, E., Clauws, P., Lamon, M., and Vennik, J., *Semicond. Sci. Technol.*, vol. 1, pp. 53, 1986.

[B21] Simoen, E., Clauws, P., and Vennik, J., *J. Appl. Phys.*, vol. 18, pp. 3041, 1985.

[B22] Simoen, E., Clauws, P., and Vennik, J., *Solid State Commun.*, vol. 54, pp. 1025, 1985.

[B23] Swierkowski, S. P., Yee, J. H., Armantrout, G. A., and Wichner, R., *J. Appl. Phys.*, vol. 45, pp. 3949, 1974.

[B24] Thurber, W. R., Forman, R. A., and Phillips, W. E., *J. Appl. Phys.*, vol. 53, 1982.

[B25] van der Pauw, L. J., *Philips Res. Rep.*, vol. 13, pp. 1, 1958.

[B26] Van Sande, M., Van Goethem, L., De Laet, L., and Guislain, H., *J. Appl. Phys.*, vol. 40, pp. 257, 1986.

[B27] Westbrook, R.D., *J. Electrochem Soc.*, vol. 121, pp. 1212, 1974.

Copyright The Institute of Electrical and Electronics Engineers, Inc.
Provided by IHS under license with IEEE
No reproduction or networking permitted without license from IHS

Not for Resale

Annex A

(informative)

This annex is not part of this standard and is included for background material only. Except for the prefix letter "A," paragraph numbers correspond to those in the main body of the text to which the material pertains.

A.5 Round-robin results of van der Pauw measurements.

The van der Pauw method allows for the measurement of ρ and R_H on lamellar samples of uniform thickness, *d*, and carrier concentration, n or p. Details of sample preparation and the methods of measurement are given in clause 5 in the main body of the text.

While use of the van der Pauw technique for analyzing HPGe is universal, each laboratory seems to have its own method of sample preparation and analysis. A round-robin measurement was conducted to determine the reproducibility and stability of the measured quantities and to see if practices could be found that would reduce the variability of the measurements.

A.5.a Surface properties

Semiconductor surfaces are characterized by surface charge density and the origin of the charge centers. Interface charge is located at the semiconductor-oxide interface and equilibrates rapidly with the free carriers in the bulk (fast states). Charged centers in the oxide may be due to stoichiometric or chemical defects (slow states). These states may equilibrate slowly (if at all) with the free carriers in the bulk of the semiconductor. In the bulk, there is an equal but oppositely charged space-charge region adjacent to the surface. The total surface charge may be such as to increase the bulk carrier density near the surface (accumulation), decrease the bulk carrier density (depletion), or create a surface layer with charge type opposite to that in the bulk (inversion). In addition, the slow states may be responsible for transients in the measured transport properties. Measurement of C^{-2} vs. *V* curves on cooled germanium detectors generally requires several minutes to stabilize at each voltage. This phenomenon is attributed to slow states. N-type surfaces are more prevalent than p-type because the former are induced by moisture. Some methods of preparation should be avoided because they ensure that surface related donors dominate bulk carriers of either type.

A.5.b Mechanics of the round-robin

Four laboratories in three different countries participated in the round-robin.

A p-type and an n-type slice were selected. The four participants measured each slice using two different preparation techniques labeled procedure A (see 5.1.3.1) and procedure B (see 5.1.3.2). Laboratories #1 and #2 also reported some results for procedure C (see 5.1.3.3). The experimental results are listed in tables A1 and A2.

To examine the importance of achieving electronic equilibrium, it was requested that, for each measurement, participants obtain one set of ρ and R_H values immediately after cooling at 77 K, and a second set 15 min later. The respective calculations of ρ and R_H are indicated by arrows. As there were significant variations between laboratories in time required to obtain the data for ρ and R_H, only general conclusions can be drawn from the magnitude of the transients. Each slice was then cut to obtain a square at the center and a square near the side. Laboratories #1 and #4 measured the squares using the same matrix of conditions described above for the original slices.

Copyright The Institute of Electrical and Electronics Engineers, Inc.
Provided by IHS under license with IEEE
No reproduction or networking permitted without license from IHS Not for Resale

Table A1—Round-robin measurements of n-type sample

Lab.	Wet-Chemical Procedure	ρ (Ω · cm)	$\lvert R_H \rvert$ (10^8 cm^3/C)	μ_H (10^4 cm^3/Vs)	$\lvert R_H/r \rvert$ (10^8 cm^3/C)	μ_H/r (10^4 cm^3/Vs)
Whole slice						
#1	A	6419 → 6488	2.20 → 2.23	3.44	2.69	4.14
	B	6085 → 6304	2.03 → 2.10	3.33	2.53	4.01
#2	A	5180 → 6480	1.79 → 2.13	3.29	2.57	3.96
	B	5970 → 6430	2.07 → 2.37	3.69	2.86	4.45
#4	A	4070 → 4660	0.98 → 1.26	2.70	1.41	3.02
	B	4110 → 4240	1.21 → 1.26	2.97	1.41	3.32
#3	A	3887 → 4080	1.26 → 1.28	3.14	1.42	3.47
	B	5404 → 5687	1.92 → 1.96	3.45	2.17	3.82
Center square						
#4	A	8000 → 8020	2.56 → 2.65	3.30	2.96	3.69
	B	5280 → 5520	1.48 → 1.61	2.92	1.80	3.26
#1	A	3946 → 8035	1.08 → 2.47	3.07	2.98	3.70
	B	4992 → 7813	1.30 → 2.39	3.06	2.88	3.69
	C	8514 → 8380	2.78 → 2.79	3.33	3.36	4.01
Side square						
#4	A	4780 → 4960	1.28 → 1.32	2.66	1.47	2.97
	B	3190 → 3300	0.83 → 0.90	2.73	1.01	3.05
#1	A	3412 → 5645	0.99 → 2.06	3.65	2.48	4.40
	B	3716 → 5434	1.04 → 1.75	3.22	2.11	3.88
	C	5730 → 5590	1.95 → 2.03	3.60	2.45	4.34

The data in tables A1 and A2 are presented in the chronological order in which the tests were performed.

In table A3, magnetic field strengths used by the participants are reported together with the values of r appropriate for these field strengths. These values were obtained from graphs prepared for this standard on the measurement of HPGe. Some transients in ρ and R_H were measured in almost all cases. The standard deviations for the ρ and R_H data for both the n-type and p-type samples were lower for the data set at the end of the transient. Higher mobilities were also generally obtained. Further analysis was conducted only on data obtained after 15 min of equilibration.

In table A4, mean values and standard deviations are shown of ρ, $\lvert R_H/r \rvert$, and μ_H/r on whole-slice measurements. Each entry in this table represents the result of eight measurements (four laboratories, two procedures each, A and B only). Two notable features of the data in table A4 are consistent with the effect of surface states on the reproducibility of the results. First, standard deviations are significantly higher for ρ and R_H measured on the n-type sample, which is expected from the tendency of germanium to develop n-type surfaces. Second, the standard deviation in μ_H/r (which equals $R_H/\rho r$) is significantly less than expected from the separate standard deviations in ρ and R_H, assuming those quantities to be unrelated. In fact, the standard deviation of μ_H/r is closer to the algebraic difference than to the quadratic sum of the standard deviations of

Copyright The Institute of Electrical and Electronics Engineers, Inc.
Provided by IHS under license with IEEE
No reproduction or networking permitted without license from IHS
Not for Resale

Table A2—Round-robin measurements of p-type sample

Lab.	Wet-Chemical Procedure	ρ (Ω · cm)	$\lvert R_H \rvert$ (10^8 cm^3/C)	μ_H (10^4 cm^3/Vs)	$\lvert R_H/r \rvert$ (10^8 cm^3/C)	μ_H/r (10^4 cm^3/Vs)
Whole slice						
#1	A	7247 → 7194	4.46 → 4.39	6.10	3.63	5.04
	B	7214 → 7143	4.51 → 4.48	6.27	3.70	5.18
#2	A	7220 → 7270	4.35 → 4.52	6.22	3.42	4.71
	B	6800 → 7340	4.19 → 4.44	6.05	3.36	4.58
	C	7760 → 7630	3.48 → 4.79	6.28	3.63	4.76
#4	A	7820 → 7375	3.76 → 3.76	5.10	3.67	4.98
	B	7330 → 7330	3.73 → 3.72	5.08	3.63	4.96
#3	A	7893 → 7899	4.30 → 4.29	5.43	4.20	5.32
	B	7717 → 7657	4.07 → 4.06	5.30	3.98	5.20
Center square						
#4	A	7370 → 7120	2.02 → 3.07	4.31	3.00	4.20
	B	8180 → 7870	3.11 → 3.28	4.17	3.20	4.17
#1	A	8376 → 6837	4.06 → 3.85	5.63	3.17	4.65
	B	6803 → 6700	3.87 → 3.87	5.78	3.20	4.78
	C	6965 → 6965	3.99 → 3.97	5.70	3.28	4.71
Side square						
#4	A	8680 → 8600	3.65 → 3.64	4.23	3.55	4.13
	B	9590 → 9220	3.42 → 3.54	3.84	3.45	3.75
#1	A	8095 → 8060	4.85 → 4.83	5.99	3.99	4.95
	B	? → 8638	? → 4.16	4.82	3.44	3.98
	C	8638 → 8337	4.72 → 4.75	5.70	3.93	4.71

Table A3—Magnetic fields used for measurements and *r* values for n-type and p-type HPGe

Lab.	B (in T)	n-Type	p-Type
#1	0.032	0.83	1.21
#2	0.106	0.83	1.32
#3	0.340	0.90*	1.03
#4	0.300	0.90*	1.02

*r depends on crystallographic orientation with respect to the current and the magnetic field vector.

the two terms, indicating statistical correlation. This is consistent with surface conditions causing the measured concentration to differ from the true bulk concentration.

Copyright The Institute of Electrical and Electronics Engineers, Inc.
Provided by IHS under license with IEEE
No reproduction or networking permitted without license from IHS

Not for Resale

Table A4—Average values and standard deviations, whole-slice measurements

Parameter	n-Type	p-Type
ρ ($\Omega \cdot$ cm)	5550 ± 1050 (18.9%)	7400 ± 250 (3.4%)
R_H (10^8 cm^3/C)	2.13 ± 0.63 (29.6%)	3.70 ± 0.28 (7.6%)
μ_H/r (10^4 cm^2/Vs)	3.94 — 0.31 (7.9%)	4.97 ± 0.25 (5.0%)

A.5.c n-Type results

A pattern shared by both the n-type and the p-type data sets is more pronounced in the n-type. Its data set is discussed first.

It is noteworthy that, in all n-type measurements using either procedure A or B, the values of both ρ and R_H increased (carrier concentration decreasing) during the transient. This is consistent with electrons freezing out on slow surface donor states after immersion into LN. The largest transients were consistently observed at laboratory #1. It is unclear whether this was due to a feature of the surfaces produced there, or whether laboratory #1 could complete a measurement faster, thereby catching more of the transient. A cursory examination of the data in table A1 indicates that which laboratory did the measurement seemed to be more relevant than which wet-chemical procedure was used. Laboratories #1 and #2 agreed fairly well using either procedure. Laboratory #3 obtained higher ρ and R_H values for procedure B, and laboratory #4 obtained higher ρ and R_H values for procedure A. In a discussion of the data, laboratory #4 provided additional data obtained with the n-type slice (see table A5).

Table A5—Supplementary data, n-type slice—laboratory #4, procedure B

ρ ($\mu \cdot$ cm)	R_H (10^8 cm^3 C^{-1})	Comment
5050	1.68	Before round-robin
4240	1.26	Round-robin
5050	1.52	New contacts after #3 measured slice

Laboratory #4, which donated the slice to the study, measured it using procedure B prior to the start of the round-robin. In addition to the measurement reported as part of the round-robin, laboratory #4 also remeasured the slice before cutting it into squares. As the repeated etching of the slice had changed the shape of the contacted area, new nicks were cut.

The data obtained by laboratory #4 using procedure A on the whole slice and also on the squares appear internally consistent, but differ sharply from the results obtained using procedures A, B, and C at laboratories #1 and #2. The latter reported higher values for ρ, R_H, and μ_H/r. Results obtained at #4 using procedure A on the squares are similar to the results obtained by #1 (higher ρ, R_H, and μ_H). It is hypothesized that the variations are due to differing contributions of n-type surface states. With this hypothesis, the higher ρ, R_H, and μ_H data are more accurate but represent only a lower bound for the true bulk electron concentration. The alternate hypothesis, that the procedure B values at laboratory #4 for ρ and R_H are more representative of the bulk, cannot definitely be eliminated; however, this hypothesis would require a p-type surface to explain the high ρ, R_H, and μ_H/r results. In this case, the reduced carrier concentration would be due to depletion of car-

Copyright The Institute of Electrical and Electronics Engineers, Inc.
Provided by IHS under license with IEEE
No reproduction or networking permitted without license from IHS
Not for Resale

riers from the surface, and the transients observed would result from increased ionization of surface acceptors, thereby producing a wider depletion region.

In summary, the significant part of the variation of the n-type data is attributed to differences in surface conditions that can be obtained at different laboratories using nominally the same procedure.

A.5.d p-Type results

Less scatter and smaller transients were observed for the p-type data than for the n-type data. Both of these observations are attributed to the electrical isolation between an n-type surface and a p-type bulk. No significant effects were observed to distinguish the results obtained with procedure A from those obtained with procedure B regarding the magnitude of measured quantities, the variation in such measurements, or the transient effects. As was the case with n-type measurements, there was less scatter among the data recorded 15 min after immersion in LN; and it is this data that was used in analysis.

A.5.e Transient effects

As with the n-type data, the wet-chemical procedure that was used had little bearing on surface-related effects, which instead were related strongly to the laboratory doing the measurement. The direction of the transients is indicated in table A6. This is a matrix including all of the measurements on p-type pieces. Upward movements are signified by "Up;" downward movements are signified by "Dn;" and no movement is signified by "0."

Table A6—p-Type data: direction of transient

Sample	Lab.	Procedure A		Procedure B	
		ρ	R_H	ρ	R_H
Slice	#1	Dn	Dn	Dn	Dn
Slice	#2	Up	Up	Up	Up
Slice	#3	0	Dn	Dn	Dn
Slice	#4	Dn	0	0	0
Center square	#4	Dn	Up	Dn	Up
Center square	#1	Dn	Dn	Dn	0
Side square	#4	Dn	Up	Dn	Dn
Side square	#1	Dn	Dn	?	?

Inspection will reveal that each laboratory displays a specific pattern. The slow surface states believed to be responsible for the transient effects appear to be specific to the laboratory rather than to the wet-chemical procedure. It is not known if this is a result of consistent variations in the implementation of the procedures or if the surfaces are altered by exposure to ambient air following the procedures. Humidity is a possible cause of such a consistent pattern.

A.5.f Mobility results

A group of calculated average drift mobilities, μ_H/r, is presented in table A7. Also included are the standard deviations and the number of measurements comprising the averages (in parentheses).

Copyright The Institute of Electrical and Electronics Engineers, Inc.
Provided by IHS under license with IEEE
No reproduction or networking permitted without license from IHS
Not for Resale

Table A7—Averages for the measured drift mobility in units of 10^4 cm^2 $V^{-1}s^{-1}$*

Sample	μ_p	μ_n
Whole slice	4.97 ± 0.25 (9)	3.94 ± 0.31 (7)
Center square	4.48 ± 0.32 (5)	3.67 ± 0.27 (5)
Side square	4.30 ± 0.51 (5)	3.73 ± 0.69 (5)
Laboratory #1, both squares	4.63 ± 0.34 (6)	4.00 ± 0.31 (6)
Laboratory #4, both squares	4.04 ± 0.20 (4)	3.24 ± 0.32 (4)
Laboratory #4, procedure B	3.91 ± 0.23 (2)	3.16 ± 0.15 (2)

*The numbers in parentheses indicate the number of measurements.

The values of mobility derived from whole-slice van der Pauw measurements are known to be distorted by the concentration gradients (see [B27]). Therefore, greater physical significance should be attached to the results on the square samples where, because of smaller sample size, concentration gradients have less impact. Analysis of these data reveals two features: first, hole drift mobilities are consistently higher than electron drift mobilities; and second, laboratory #1 obtained higher mobilities for both holes and electrons than did laboratory #4. Both stated that the results obtained and listed in table A7 are typical of their routine measurements. At laboratory #4, concentrations were calculated from measured resistivities based on the assumed drift mobilities of μ_n = 36 000 cm^2 $V^{-1}s^{-1}$ (see [B9]) and μ_p = 42 000 cm^2 $V^{-1}s^{-1}$ (see [B10]). These values are in the detector literature (see [B18]). Later work on HPGe reported that $\mu_n = \mu_p$ = 45 000 cm^2 $V^{-1}s^{-1}$ and $\mu_n = \mu_p$ = 44 000 cm^2 $V^{-1}s^{-1}$. Laboratory #1 normally calculates concentrations from R_H ($|N_A - N_D| = r/qR_H$) and uses ρ only to calculate μ, which is considered indicative of the quality of the measurement or the uniformity of the sample.

There are several possible causes of the systematic discrepancies in the determination of mobility, but errors in the thickness measurement and calibration factors for the voltage and current determinations are not among them because they cancel in the calculation. Possible sources of error that remain are

a) Uniformity and magnitude of B
b) Magnitude of r
c) Effects of surface states

The first two affect only the values of R_H/r; but inspection of table A2 (p-type data) reveals that laboratories #1 and #2 are in better agreement on R_H/r than on ρ. The lower mobilities measured at laboratory #4 are due more to relatively higher ρ values than to relatively lower R_H/r, although both factors contribute.

A.5.g Determination of impurity concentration

There are three issues in the determination of impurity concentration:

a) How to prepare the sample
b) Whether to use ρ or R_H in calculating concentrations
c) What material parameters to use (μ, r)

Accuracy of ±10% would be useful to detector makers in projecting depletion voltages. The reproducibility of ρ and R_H measurements at different laboratories was within that limit for p-type samples but not for n-type samples. In the most extreme case, a factor of two difference in R_H was observed in the n-type side

Copyright The Institute of Electrical and Electronics Engineers, Inc.
Provided by IHS under license with IEEE
No reproduction or networking permitted without license from IHS
Not for Resale

square between laboratories #1 and #4. In these circumstances, it seems prudent to allow some flexibility in wet-chemical procedures in order to accommodate differing ambient environmental effects on surface states. It should be required that processing details be provided if requested by a user. A standard for measuring HPGe should contain a suggested wet-chemical procedure that would be least likely to present difficulties to someone who is nonroutinely performing van der Pauw measurements. Procedure B has the advantage that it does not require mixing acid with methanol, which may present disposal problems in some circumstances.

In a uniform sample with no net surface charge, the concentration calculated from ρ should be the same as that calculated from R_H, if μ and r are known accurately. In the presence of concentration gradients, micro-inhomogeneities, and differing surface states, measurements will vary. Which average is most useful is left in doubt. Obtaining concentrations by ρ has the advantage that it does not depend on accurate measurement of the magnetic field; but it has the disadvantage that there seems to be more controversy about the values of μ than of r. Under the circumstances, it is recommended that the choice of method be left to the measuring laboratory. However, if the ρ technique is employed, the lower values for μ (μ_p = 42 000 cm^2 V^{-1} s^{-1}, μ_n = 36 000 cm^2 V^{-1}s^{-1}) should be used because they will yield higher calculated concentrations, thereby better serving the interests of the user. If the concentration is obtained from R_H, the r values specified in this standard should be used.

A.5.h Conclusions: round-robin tests

a) Standard deviations for measurements of ρ and R_H/r were less than 10% for the p-type slice and less than 30% for the n-type slice.

b) The limiting factor in accuracy and reproducibility was control of surface states. These seemed to be specific to a particular laboratory rather than to the wet-chemical procedure that was used. It is essential that transients be allowed to stabilize before measured values are recorded.

c) Wet-chemical procedure A (see 5.1.3.2) is suggested but is not required. Drift mobilities and r values are provided to allow for calculation of concentration from measurements of either resistivity or Hall coefficient.

d) Future work to identify a wet-chemical procedure that "travels well" would be beneficial. Also, a more directed project to accurately measure μ_p and μ_n at 77 K would resolve a current discrepancy.

A.5.2.8.2 Factor *r* in p-type HPGe

Calculations (see [B5]) indicate that when the magnetic field is low in p-type germanium, r depends critically on the ratio between impurity scattering and acoustic lattice scattering in the regime in which lattice scattering is dominant (see figure 2 of [B5]). Because this is precisely the regime for HPGe at 77 K, there was concern that r might depend on the concentration of residual defects. To address this issue, van der Pauw measurements were made on samples of varying ($N_A - N_D$) values and at regular magnetic field intervals up to 0.18 T. No such effect was observed for hole concentrations between 10^{10} and 10^{13} cm^{-3}. [The r values specified in figure 5.3 b) were derived from this study.] The most likely reason for this is the neglect of optical lattice scattering in [B5]. When this phenomenon is considered, it has the effect of damping out large increases in r due to small residual impurity scattering. While explicit calculations are not presented in [B23], it was concluded that for $B < 0.1T$ and $T > 70$ K, optical scattering should be taken into account. The experimentally determined magnetic field correction for r in p-type HPGe at 77 K is given in figure 5.4 (see 5.2.8.2).

Copyright The Institute of Electrical and Electronics Engineers, Inc.
Provided by IHS under license with IEEE
No reproduction or networking permitted without license from IHS
Not for Resale

ISBN 1-55937-298-2

Copyright The Institute of Electrical and Electronics Engineers, Inc.
Provided by IHS under license with IEEE
No reproduction or networking permitted without license from IHS

Not for Resale